

**UCLA**

**UCLA Previously Published Works**

**Title**

Variations between foundation-level and free-field earthquake ground motions

**Permalink**

<https://escholarship.org/uc/item/0cx1452c>

**Journal**

Earthquake Spectra, 16(2)

**Author**

Stewart, Jonathan P

**Publication Date**

2000

Peer reviewed

# Variations between Foundation-Level and Free-Field Earthquake Ground Motions

Jonathan P. Stewart, M.EERI

Strong motion data from sites having both an instrumented structure and free-field accelerograph are compiled to evaluate the conditions for which foundation recordings provide a reasonably unbiased estimate of free-field motion with minimal uncertainty. Variations between foundation and free-field spectral acceleration are found to correlate well with dimensionless parameters that strongly influence kinematic and inertial soil-structure interaction phenomena such as embedment ratio, dimensionless frequency (i.e., product of radial frequency and foundation radius normalized by soil shear wave velocity), and ratio of structure-to-soil stiffness. Low frequency components of spectral acceleration recorded on shallowly embedded foundations are found to provide good estimates of free-field motion. In contrast, foundation-level peak ground acceleration (both horizontal and vertical) and maximum horizontal velocity, are found to be de-amplified. Implications for ground motion selection procedures employed in attenuation relations are discussed, and specific recommendations are made as to how these procedures could be improved.

## INTRODUCTION

Empirical attenuation relationships, evaluated using regression analyses on various indices of recorded ground motions, are often used to estimate ground motion for a given set of design conditions (e.g., site-source distance, source magnitude and mechanism, site condition). Authors of many commonly used relationships (e.g., *Seismological Research Letters*, 1997) typically select from the world-wide ground motion inventory seismograms that are unlikely to be subject to significant contamination from soil-structure interaction for use in their regression. The intent is to develop relationships for free-field conditions, which requires the omission of motions influenced by vibrations of structures such as buildings, bridges, or dams. Such omissions significantly affect database size, particularly limiting data from older earthquakes for which recordings are largely from the foundation levels of buildings.

This paper will make use of strong motion data recorded at sites with instrumented building structures and free-field accelerographs to examine variations between free-field and foundation-level ground motion indices. The intent is to critically assess ground motion selection procedures used in several modern attenuation relations, and to suggest modifications to these procedures. The approach taken is to (1) identify critical parameters found from previous soil-structure interaction (SSI) studies to affect variations in the Fourier spectral amplitudes of foundation and free-field motions, (2) measure the effects of these SSI parameters on variations in motion indices commonly used in attenuation relations such as Maximum Horizontal/Vertical Acceleration (MHA/MVA), 5%-damped spectral acceleration at various periods, and Maximum Horizontal Velocity (MHV), and (3) compare the ground

---

Dept. of Civil & Environmental Engineering, University of California, Los Angeles, CA 90095-1593

motion variations found in Step 2 with the variations obtained using parameters currently employed in ground motion selection procedures for attenuation relations.

Empirical approaches that have been used previously to investigate SSI effects on ground motion include: (1) the present approach of comparing recordings from nearby buildings of different sizes, including instrument shelters (e.g., Housner, 1959; Duke et al., 1970; Crouse and Jennings, 1975; Boore et al., 1980; Seed and Lysmer, 1980; McCann and Boore, 1983; Campbell, 1984a), (2) regression analyses for attenuation relations that include a structural parameter, and utilize a strong motion database which includes structural recordings (Campbell, 1984a, 1984b), and (3) comparisons of normalized Fourier amplitude spectra of recordings from buildings of different sizes (Lee et al., 1982; Moslem and Trifunac, 1987). Some of the principal conclusions from these studies include:

1. The amplitude of strong motion recordings decreases with embedment depth (e.g., Crouse and Jennings, 1975; Seed and Lysmer, 1980; McCann and Boore, 1983; Campbell, 1984a; Chang, et al., 1985).
2. Spectral amplitudes of ground motion are not significantly dependent on foundation size, i.e., observed variations of spectral content with foundation size were within the scatter of the data, as represented by confidence intervals (Lee et al., 1982; Moslem and Trifunac, 1987).
3. Ground motions from the base of buildings decrease with increasing building height (Boore et al., 1980; Campbell, 1984b).

It should be noted at this point that these factors (embedment depth, foundation size, building height) do not provide a complete nor a rigorous quantification of soil-structure interaction processes. Nonetheless, the findings from many of these previous studies comprise the basis for ground motion selection procedures used in many attenuation relationships. One such procedure (commonly known as the "Geomatrix" procedure) is summarized in Table 1 and can be stated as follows:

Data from structures with more than two to three stories are not used.

Data from short (< 2-3 story) structures are used if there is no basement, or if there is a single-level basement with a non-massive foundation. Data recorded in single-level basements with massive foundations are used only for rock site conditions.

Data recorded at the base of multi-level basements are not used. However, data recorded at the ground level are used provided the building is low-lying above the ground line (<2-3 stories) and the foundation is not massive.

According to Silva (1998, *personal communication*), the Geomatrix procedure was invoked during the development of the databases used by Sadigh et al. (1997), Abrahamson and Silva (1997), and Idriss (1991). Other investigators have used different criteria. For example, Campbell (1997) neglects all data recorded in basements, and neglects data from buildings with > 2 stories and > 5 stories which are founded on soil/soft rock and hard rock, respectively. Boore et al. (1997) include data from embedded structures, but neglect all data from buildings with > 3 stories. Trifunac and his coworkers used records from the base of buildings in early versions of their attenuation relations (Trifunac, 1976a,b). In their more recent relations (Lee and Trifunac, 1996), building records were selected based on judgement, with relatively few being selected (Todorovska, 1999, *personal communication*).

**Table 1.** Criteria for use of foundation recordings for attenuation relations

Investigator	Basement	# Stories Criteria
“Geomatrix Criteria” (Sadigh et al., 1997; Abrahamson and Silva, 1997; Idriss, 1991)	Neglect if single level basement, massive foundation, soil Neglect all multiple level basement	>2 to 3 stories neglected
Campbell (1997)	All Neglected	> 2 stories neglected (soil, soft rock) >5 stories neglected (hard rock)
Boore et al. (1997)	Included	≥ 3 stories neglected
Trifunac Group (see text)	See text	See text

This paper expands upon the previous work in two ways. First, variations in ground motion between the foundation and free-field are correlated to a different set of parameters than those invoked previously. The selected parameters are intended to provide a more physically-based representation of SSI effects. Each parameter used here has been shown to influence foundation/free-field transfer functions from analyses (by others) of simplified soil-foundation-structure systems, and has also been verified as a reasonable indicator of SSI effects from previous studies of field performance data. Second, the ground motion variations are evaluated from a much larger data set of nearby building/free-field recordings than had been available in the previous studies.

## DATABASE

### SITE SELECTION

All sites considered in this study have a free-field accelerograph and a structure instrumented to record foundation-level translations. Most sites also have recordings of roof translation, which enable the identification of the structure’s apparent modal vibration periods and damping ratios. Each site was reviewed for the following: (1) the free-field instrument is not so close to the structure as to be significantly affected by structural vibrations; and (2) the free-field instrument is not so far from the structure that free-field and foundation-level motions exhibit significant incoherence at the first-mode frequency of the structure. The latter criteria is enforced to enable meaningful analyses of variations between free-field and foundation motions that result from building vibrations. The procedures by which these checks were made are summarized as follows:

- Possible contamination of free-field motion from structural vibrations is checked using power spectral density and coherency functions for the free-field and foundation motions. High coherencies between the two motions at modal frequencies, or spectral peaks in free-field motions at modal frequencies, indicate potential contamination. Sites failing such checks were not used.
- Potential incompatibility of foundation and free-field motions resulting from excessive spatial incoherence was investigated using the empirical models developed by Abrahamson et al. (1991) and Abrahamson (1988) from data recorded at the Lotung, Taiwan LSST array and SMART1 array, respectively. Based on these models and a minimum acceptable coherency of 0.8, free-field/structure separations were required to be

less than about 800 m for 1 Hz structures, 450 m for 2 Hz structures, and 150 m for 4 Hz structures. Free-field/structure pairs with greater separations were not considered. Coherency functions for sites meeting these criteria were generally found to be acceptable.

Note that incoherence effects at frequencies higher than the first-mode frequency are not controlled by these criteria, which should enhance scatter in comparisons of free-field and foundation-level ground motion indices that are sensitive to high frequency components of motion (such as peak ground acceleration). This will be examined subsequently in the paper.

Using the above criteria, suitable free-field instruments were sought for virtually all instrumented structures in California, and 44 were identified (plus one additional structure in Taiwan).

### SITE CONDITIONS

The 45 sites considered in this study are listed in Table 2. For the 45 sites, 64 processed data sets are available as a result of multiple earthquake recordings at 14 sites. Fifteen California earthquakes contributed data to this study, the most significant of which are the  $M_W = 6.0$  Whittier,  $M_W = 6.9$  Loma Prieta,  $M_W = 5.6$  Upland,  $M_W = 7.0$  Petrolia,  $M_W = 7.3$  Landers, and  $M_W = 6.7$  Northridge earthquakes. The maximum horizontal accelerations (MHAs) occurring at the sites during these earthquakes are  $> 0.6g$ , 1 data set;  $0.4-0.6g$ , 4 data sets;  $0.2-0.4g$ , 22 data sets;  $0.1-0.2g$ , 7 data sets;  $< 0.1g$ , 30 data sets. The maximum horizontal velocities (MHVs) are  $> 40$  cm/s, 4 data sets;  $20-40$  cm/s, 11 data sets;  $10-20$  cm/s, 16 data sets; and  $< 10$  cm/s, 33 data sets. Hence, moderate- and low-level shaking is well represented in the database, but data for intense shaking ( $MHA > 0.4g$ ) is relatively sparse (only 5 data sets).

The shear wave velocities indicated in Table 2 are the ratio of effective profile depth to the small strain shear-wave travel time through the profile. The effective profile depth is taken as the foundation radius  $r = \sqrt{A_f/\pi}$ , where  $A_f$  = area of foundation. This profile depth is chosen because it has been found to provide a good representation of soil stiffness for use in the evaluation of inertial interaction effects (Stewart and Kim, 1998). Site specific small-strain shear-wave velocity profiles for the sites are given in Stewart and Stewart (1997), although supplemental data have been obtained for several sites since that publication. Site 19 is omitted from the compilation because data did not become available by the time this paper was prepared.

### DATA PROCESSING

The strong motion data used in this study was acquired from the California Strong Motion Instrumentation Program, the U.S. Geological Survey, the University of Southern California, the Pacific Gas and Electric Company, and the Electrical Power Research Institute. The instrument owners generally performed the data digitization and processing, and further processing was not performed for this study unless the structure and free-field time steps differed. In such cases, the data with the finer time step was decimated to match the data with the coarser time step. Decimation was performed by first low-pass filtering the data with a corner at the desired new Nyquist frequency (8th order low-pass Chebyshev-type I filter), and then re-sampling the resulting smoothed signal at the specified lower rate.

Table 2. Data for sites included in this study

Site	Station	No. Eqs.	Rock/Soil	Avg. $V_s$ (m/s)*	Piles (Y/N)	Embed. (m)	r (m)	No. Stories	Period (s)	$r/e$	$\frac{1}{\alpha}$ Eq. 2	$\frac{\bar{\alpha}_0}{\omega}$ Eq. 4 x10 (s)	$\kappa$	FF-Str. Sep. (m)
1	Eureka Silvercrest Apts.	1	S	244	N	0	17	5	0.2	0.00	0.19	0.17	0.09	104
2	Fortuna 1-St. Supermarket	2	S	279	N	0	35	1	0.4	0.00	0.06	0.35	0.03	107
3	Humboldt Bay Power Plant	2	S	299	N	26	18	1	na	1.43	na	0.18	na	73
4	Emeryville Pacific Pk. Plaza	1	S	189	Y	0	27	31	2.5	0.00	0.14	0.27	0.09	162
5	Hayward City Hall	1	R	674	Y	0	20	11	1.2	0.00	0.03	0.20	0.22	143
6	Hayward 13-St. School Bldg.	1	R	411	Y	0	19	13	1.3	0.00	0.08	0.19	na	384
7	Hollister 1-St. Warehouse	1	S	204	N	0	30	1	0.7	0.00	0.06	0.30	0.07	122
8	Piedmont Jr. High School	1	R	558	N	0	16	3	0.2	0.00	0.07	0.16	0.24	37
9	Pleasant Valley Pump. Plant	2	S	277	N	10	16	1	0.5	0.60	0.11	0.16	na	91
10	Richmond City Hall	1	S	253	N	3	23	3	0.3	0.13	0.13	0.23	0.14	198
11	San Jose 3-St. Offc. Bldg.	1	R	820	N	0	26	3	0.7	0.00	0.02	0.26	0.62	155
12	El Centro Imp. Co. Serv. Bldg.	1	S	177	Y	0	19	6	0.7	0.00	0.13	0.19	0.05	104
13	Indio 4-St. Govt. Offc. Bldg.	1	S	232	Y	5	21	4	0.7	0.22	0.11	0.21	na	73
14	Lancaster 3-St. Offc. Bldg.	1	S	280	Y	0	16	3	0.2	0.00	0.14	0.16	0.34	76
15	Lancaster 5-St. Hosp.	1	S	314	Y	0	30	5	0.7	0.00	0.06	0.30	0.12	110
16	Lancaster Fox Airfield	1	S	305	N	0	4	5	0.3	0.00	0.15	0.04	na	49
17	Loma Linda VA Hosp.	1	S	463	Y	0	75	4	0.3	0.00	0.11	0.75	0.11	122
18	Long Beach Har. Ad. Bldg.	1	S	213	Y	0	15	7	1.4	0.00	0.06	0.15	0.09	61
20	Long Beach VA Hosp.	1	S	369	N	7	26	11	0.6	0.27	0.13	0.26	0.15	299
21	LA 2-St. FCCB	3	R	314	N	0	22	2	0.8	0.00	0.03	0.22	0.2-0.4	30
22	LA 3-St. Comm. Bldg.	1	S	354	N	7	40	3	0.6	0.17	0.07	0.40	na	518
23	LA 6-St. Offc. Bldg.	1	S	192	N	4	7	5	0.9	0.65	0.10	0.07	na	253
24	LA 6-St. Pkg. Garage	1	S	265	Y	0	48	6	0.5	0.00	0.09	0.48	0.06	73
25	LA 7-St. USC Hosp.	2	R	357	N	0	34	7	1.2	0.00	0.05	0.34	0.13	107
26	LA 7-St. UCLA Bldg.	1	S	213	N	4	10	7	0.7	0.41	0.13	0.10	na	283
27	LA 15-St. Offc. Bldg.	2	R	360	N	0	40	17	3.1	0.00	0.05	0.40	0.08	229
28	LA 19-St. Offc. Bldg.	1	S	354	Y	12	28	19	3.2	0.41	0.06	0.28	na	287
29	LA Hollywood Storage Bldg.	4	S	293	Y	3	18	14	2.2	0.15	0.05	0.18	0.6	43
30	LA Wadsworth VA Hosp.	1	S	452	Y	9	58	6	0.9	0.16	0.06	0.58	0.08	143
31	Newport Beach Hoag Hosp.	1	S	320	N	0	19	11	0.9	0.00	0.10	0.19	na	198
32	Norwalk 12400 Imp. Hwy.	1	S	277	Y	4	28	7	1.5	0.15	0.05	0.28	0.13	149-174
33	Norwalk 12440 Imp. Hwy.	2	S	305	Y	5	43	7	1.3	0.11	0.06	0.43	0.03	40-201
34	Palmdale 4-St. Hotel	1	S	494	N	0	21	4	0.2	0.00	0.07	0.21	0.16	73
35	Pomona 2-St. Bldg.	2	S	390	Y	3	18	2	0.3	0.18	0.07	0.18	0.3	88
36	Pomona 6-St. Bldg.	2	S	381	N	4	15	6	1.2	0.25	0.04	0.15	na	387
37	Rancho Cucamonga LJC	5	S	420	N	4	37	4	0.6	0.12	0.07	0.37	0.1	101
38	San Bernardino 3-St.	1	S	299	N	0	24	3	0.6	0.00	0.05	0.24	na	210
39	San Bernardino 5-St.	1	S	399	N	4	29	5	0.6	0.14	0.07	0.29	0.13	149
40	San Bernardino Vanir Tower	1	S	280	Y	0	17	9	2	0.00	0.04	0.17	0.13	277
41	San Bernardino Co. Govt. Ctr.	1	S	323	Y	0	35	5	0.5	0.00	0.07	0.35	0.05	64
42	Santa Susana Bldg. 462	1	R	1372	N	0	7	8	0.6	0.00	0.03	0.07	na	49
43	Seal Beach Rockwell Bldg. 80	2	S	296	Y	5	31	8	1.3	0.16	0.07	0.31	0.00	140
44	Sylmar Olive View Med. Ctr.	2	S	466	N	0	38	6	0.3	0.00	0.14	0.38	0.07	140
45	Ventura 12-St. Hotel	1	S	280	Y	0	19	12	0.7	0.00	0.11	0.19	0.00	55
46	Lotung Containment Structure	1	S	140	N	5	5	1	0.5	0.92	0.20	0.05	na	30

\* Shear wave velocities in *italics* are estimated (Stewart and Stewart, 1997).

\*\* Strain factor = PGV/Vs (PGV taken from average horizontal component), Trifunac and Todorovska, 1996.

## FACTORS INFLUENCING VARIATIONS BETWEEN FOUNDATION AND FREE-FIELD MOTION

It is widely known that soil-structure interaction can modify foundation-level motions relative to free-field motions (Kramer, 1996; Chopra, 1995), with both amplification and de-amplification of foundation-level motion possible across different frequency ranges. Two mechanisms of SSI generate the deviations between foundation and free-field motions:

*Inertial Interaction:* Inertia developed in the structure due to its own vibrations gives rise to base shear and moment, which in turn cause displacements and rocking of the foundation relative to the free-field. These relative displacements can lead to amplification of foundation-level motion relative to the free-field at the fundamental-mode flexible-base period of the structure ( $\tilde{T}$ ).

*Kinematic Interaction:* Three kinematic effects can reduce foundation motions relative to the free-field, each of which tends to become more pronounced with increasing frequency. First, an assemblage of stiff foundation elements located on or in soil moves as a constrained body. Since free-field motions are spatially and temporally incoherent, motions on surface foundations are filtered with respect to free-field motions. This “base slab averaging” was first noted by Yamahara (1970) and later by Scanlan (1976) and Newmark et al., (1977). Second, embedded foundations are subject to ground motion filtering associated with the variation of ground motion amplitude with depth. Third, scattering of seismic waves off of corners on the foundation can further reduce foundation motions at high frequencies (Trifunac, 1971).

At a site with recordings of both free-field and foundation-level motions, variations between these motions result from a composite of kinematic and inertial effects, as well as random variations resulting from spatial incoherence effects.

Figure 1 compares MHA and spectral acceleration at the first-mode building period ( $S_a @ \tilde{T}$ ) for the full data set, which includes motions in the transverse and longitudinal directions for most structures and earthquakes. The MHA data in Figure 1a generally indicate de-amplification of foundation-level MHA, and a perceptible increase in the level of de-amplification with increasing MHA. The MHA de-amplification can be attributed to either kinematic interaction (which is most pronounced at high frequencies) or localized soil nonlinearities beneath the foundation. It should be noted that the nonlinearity that would affect the de-amplification shown in Figure 1 is not the nonlinearity associated with free-field ground response (which would affect both the structure and free-field essentially identically). Rather, the nonlinearity referred to here results from localized stresses in the soil beneath the foundation associated with the structure’s base shear and moment.

In Figure 1a, the increase of MHA de-amplification with MHA suggests that soil nonlinearity may be affecting the data. The variation of MHA de-amplification with a strain parameter (i.e., strain factor =  $PGV/V_s$ , as defined by Trifunac and Todorovska, 1996) is shown in Figure 1b. The level of de-amplification is not seen to increase with strain factor. This result is not surprising because strain factor is a measure of free-field strain, which would not be expected to correlate well to soil nonlinearities associated with structural vibrations. Such nonlinearities would be expected to be sensitive to building mass (related to number of stories), spectral acceleration at the first-mode building period (i.e.,  $S_a @ \tilde{T}$ ), and the amount of inertial soil-structure interaction. These effects are examined subsequently in the paper.

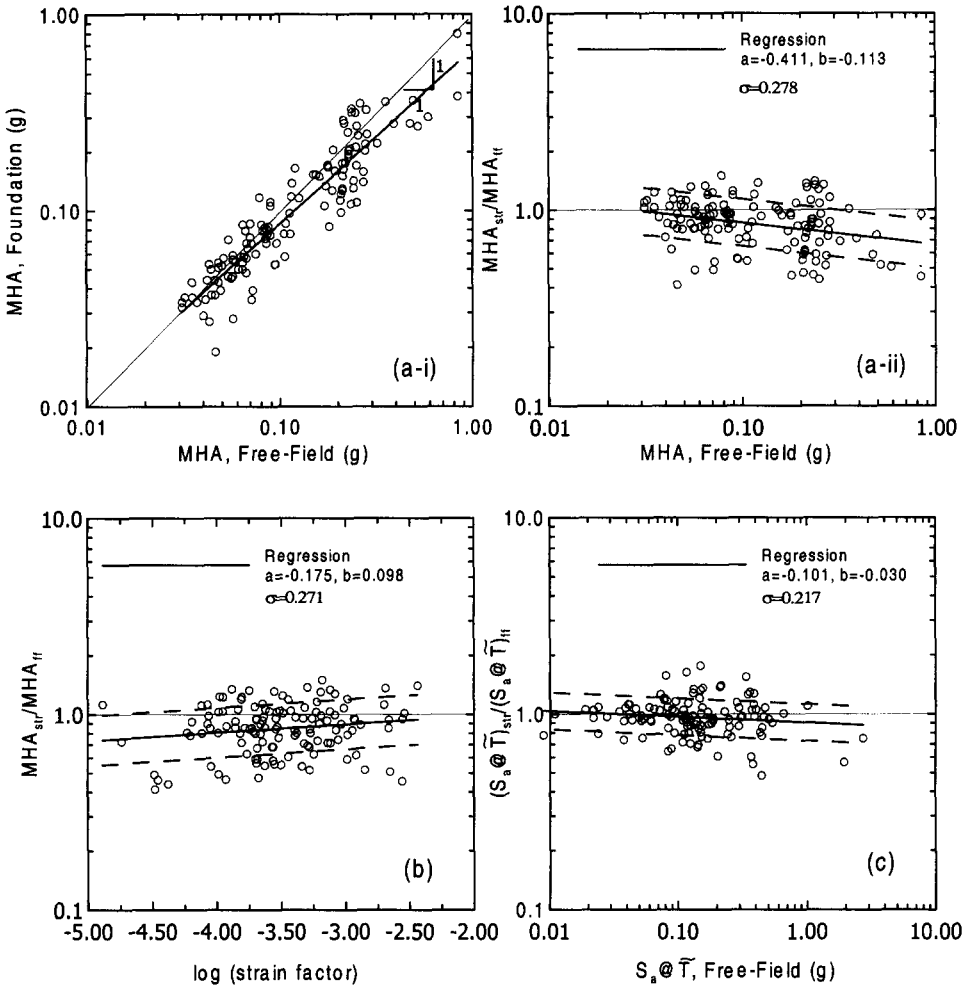


**Figure 1.** (a)-(b) Variation between free-field and foundation-level MHA, full data set; (c) variation in 5% damped spectral acceleration at building period, full data set.

The de-amplification of the  $S_a @ \tilde{T}$  data is shown in Figure 1c. Significantly less de-amplification is observed than in the MHA data, which may result from both foundation motion amplification associated with inertial interaction (which is most pronounced at  $\tilde{T}$ ), and the reduced kinematic effect at longer spectral periods.

In order to elucidate trends in the data plotted in Figure 1, linear regression analyses were performed to fit an equation of the following form to the data,

$$\ln(\text{ratio}) = a + b \ln(\text{ff}) \tag{1}$$

where *ratio* is the ratio of foundation/free-field motion and *ff* is the amplitude of the free-field motion. Results of this regression are plotted in Figure 1. More complex equation forms were investigated, but did not significantly reduce residuals.

The residuals between the natural log of the data and regression resulting from Equation 1 are plotted in Figure 2. The residuals are essentially normally distributed (Figure 2a), and do



not vary significantly with the structure/free-field separation distance (Figure 2b). Based on Figure 2a, the standard error of the regression, denoted as  $\sigma$ , is computed from the variation between the natural log of the data and the regression, with the results listed in Figure 1. Regression results  $\pm \sigma$  are plotted in Figure 1 as dashed lines. It may be noted that the error term for MHA ( $\sigma=0.278$ ) exceeds that for  $S_a @ \tilde{T}$  ( $\sigma=0.217$ ), suggesting a higher level of data noise at high frequencies where spatial incoherence effects are most pronounced.

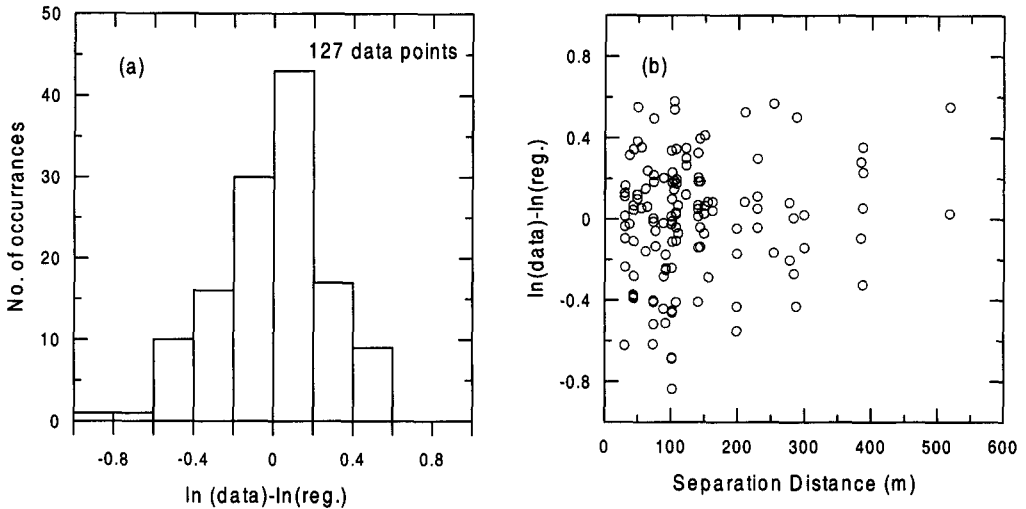


**Figure 2.** (a) Residuals between natural log of foundation/free-field data and regression, (b) variation of residual with free-field/structure separation distance.

Previous soil-structure interaction research has identified several parameters that influence kinematic and inertial interaction effects and hence foundation/free-field ground motion variations. The following three sections sub-divide the data set used in Figure 1 according to ranges of parameters describing embedment, inertial interaction, and base slab averaging effects. The parameters describing these effects were developed by others from analyses of idealized soil-foundation-structure systems. These parameters are used as indices of the respective SSI effects, and their use is not meant to imply that the idealized conditions assumed in the analyses are present in the field. The ground motion parameters that are regressed upon include MHA (which is a high frequency ground motion parameter and hence should be sensitive to kinematic interaction effects),  $S_a @ \tilde{T}$  (which is most sensitive to inertial interaction effects), and 5% damped spectral accelerations at various periods. Although Fourier spectral amplitudes are affected by the aforementioned SSI phenomena more directly than spectral accelerations,  $S_a$  is used here because of its use in attenuation relations. Hence, a measure of SSI effects on  $S_a$  is obtained to establish more rigorous time history selection procedures for attenuation relations.

## EMBEDMENT

Elsabee and Morray (1977) and Day (1978) found from finite element analyses of cylindrical embedded foundations subject to vertically incident shear waves that the de-amplification of foundation translation at a particular frequency ( $f$ ) is principally related to the fundamental frequency of the embedded layer, which is denoted here as  $f_1 = V_{s,e}/4e$  (where  $e$  = embedment depth and  $V_{s,e}$  = average shear wave velocity over depth  $e$ ). The transfer

functions predicted by these and similar analysis procedures have been verified by Kurimoto and Iguchi (1996) and Stewart (1996). To investigate the effect of embedment on foundation/free-field ground motion variations, the database was sorted using  $ff_1$  and the number of embedded stories (NES). The NES sort was motivated by its use in current strong motion selection procedures for attenuation relations.

To investigate the effect of NES on foundation/free-field ground motion variations, the database is sorted into NES = 0, 1 and > 1 in Figure 3a. Regressions according to Equation 1 are also plotted in Figure 3a, and indicate a significantly higher level of de-amplification for NES = 1 than NES = 0. However, results for NES > 1 are mixed, showing less de-amplification than NES = 1 results for MHA, but greater de-amplification for  $S_a @ \tilde{T}$ . These mixed results, coupled with the lack of a theoretical basis for relating NES to de-amplification, suggest NES may not be the optimal parameter for representing embedment effects.

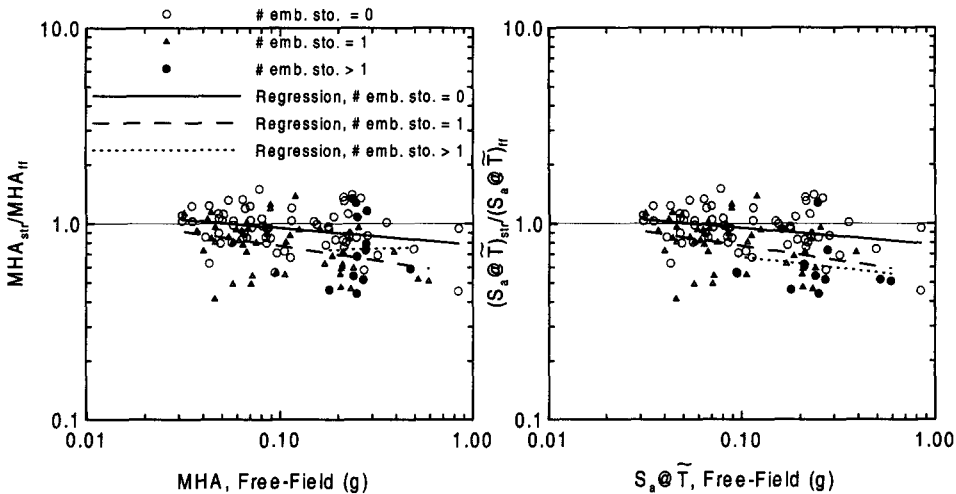


**Figure 3(a).** Ratio of foundation-level/free-field motion, complete data set, sorted by number of embedded stories (NES).

The effect of  $ff_1$  on de-amplification was investigated using spectral ordinates at  $f = 0.33, 0.56, 1.0, 1.8, 3.1,$  and  $5.6$  Hz. The resulting range of  $ff_1$  values is 0 to 2.7. Foundation-level and free-field 5% damped spectral accelerations computed at these same spectral periods are compiled in Figure 3b along with regression results according to Equation 1 for  $ff_1 < 0.1, ff_1 = 0.1-0.3,$  and  $ff_1 > 0.3$ . Figure 3c shows regression results without the data for various ranges of  $ff_1$ . The results indicate that for  $ff_1 < 0.1$ , ratios of foundation/free-field spectral ordinates are nearly unity. De-amplification occurs for  $ff_1 > \sim 0.1$ , but this de-amplification does not increase as  $ff_1$  increases. The weak correlation between de-amplification and  $ff_1$  for  $ff_1 > \sim 0.1$  suggests that factors other than embedment depth may be influencing the de-amplification.

The inconsistent trends in the results obtained for data sorted according to NES and  $ff_1$  motivated an additional data sort according to embedment ratio,  $e/r$ , where  $r$  is the radius of an equivalent circular foundation. Figure 3d compares ratios of MHA and  $S_a @ \tilde{T}$  data sorted according to  $e/r = 0, e/r > 0 \ \& \ < 0.5,$  and  $e/r > 0.5$  along with regression results fitting Equation 1 for the different data bins. The  $S_a @ \tilde{T}$  data for  $e/r > 0 \ \& \ < 0.5$  has negligible

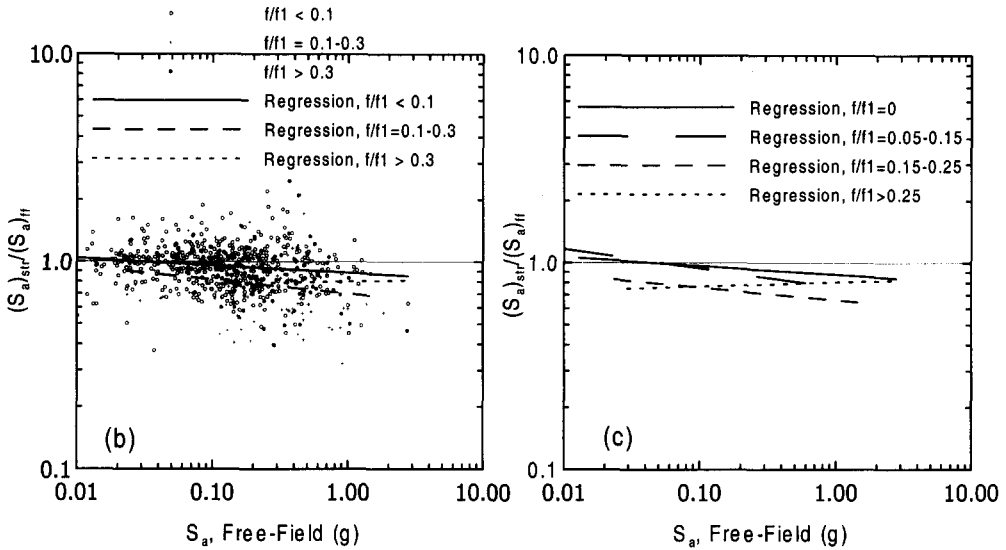


Figure 3(b-c). Ratio of foundation-level/free-field motion, complete data set, sorted by  $ff_1$ .

deviations from the  $e/r = 0$  data. The MHA deviations for these two  $e/r$  bins are larger, but are still modest. Although the data for  $e/r > 0.5$  is sparse, significant and consistent de-amplification is apparent both in MHA and  $S_a@T$  relative to  $e/r < 0.5$ . Therefore, it appears that  $e/r$  is an index that correlates well with foundation motion de-amplification, and that data with “large”  $e/r$  should be excluded from data sets. One possible explanation for the more consistent de-amplification trends observed in sorts using  $e/r$  is an increase of wave scattering effects with increasing  $e/r$ . Since scattering occurs off of corners on foundations, it would not be expected to correlate well to parameters based on embedment depth alone (i.e., NES,  $ff_1$ ) that provide no information on foundation width (i.e., the relative “closeness” of corners).

The effect of the  $ff_1$  and  $e/r$  sorting on data scatter is summarized in Table 3. The error terms for MHA indicate that data scatter for unembedded foundations ( $e/r = 0$ ) is smaller than that for the overall data set and shallowly embedded foundations ( $e/r > 0$  &  $< 0.5$ ). Conversely, error terms for the  $S_a@T$  data indicate that error terms for  $e/r = 0$  and  $e/r > 0$  &  $< 0.5$  are both smaller than the error term for the full data set. These results suggest that the most consistent comparisons of foundation and free-field ground motions are obtained for  $e/r = 0$  and  $e/r < 0.5$  for MHA and  $S_a@T$ , respectively. Using the  $ff_1$  criteria, scatter is minimized for  $ff_1 \sim 0.1$ .

Kinematic effects associated with embedment are a function of both  $ff_1$  and  $e/r$ . However, based on the above,  $e/r$  appears to provide the most consistent representation of foundation motion de-amplification. A cutoff value of  $e/r < 0.5$  is recommended for use in attenuation relations. It is acknowledged, however, that an alternative screen could be defined using  $ff_1 < 0.1$  that would also ensure minimal de-amplification.

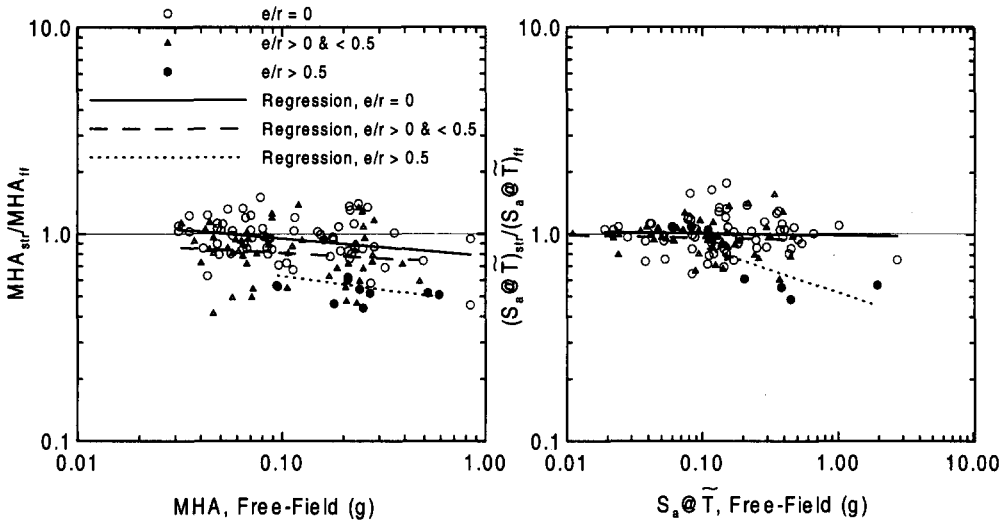


Figure 3(d). Ratio of foundation-level/free-field motion, complete data set, sorted by  $e/r$ .

Table 3. Error terms for different embedment data bins

Bin	# data pts.	$\sigma$ (MHA)	$\sigma$ ( $S_a @ \tilde{T}$ )	$\sigma$ ( $S_a$ )
Full data set	127	0.278	0.217	--
Full data set	750	--	--	0.261
$ff/f_1 = 0$	392	--	--	0.229
$ff/f_1 = 0.05-0.15$	104	--	--	0.232
$ff/f_1 = 0.15-0.25$	54	--	--	0.276
$ff/f_1 > 0.25$	76	--	--	0.382
$e/r = 0$	63	0.227	0.206	--
$e/r > 0 \ \& \ < 0.5$	54	0.286	0.190	--
$e/r > 0.5$	10	0.198	0.222	--
$e/r < 0.5$	117	0.267	0.200	--

**INERTIAL INTERACTION**

Veletsos (1977) investigated inertial interaction effects in buildings by developing analytical solutions to the response of a single degree-of-freedom structure of height  $h$  and fixed-base period  $T_s$  founded on a disk foundation of radius  $r$  which rests on the surface of a visco-elastic halfspace with shear wave velocity  $V_s$ . Veletsos' results suggest that the lengthening of first-mode building period ( $\tilde{T}/T_s$ , where  $\tilde{T}$  = flexible-base period of building) that results from inertial interaction increases with the dimensionless ratio of structure-to-soil stiffness,

$$\frac{1}{\sigma_s} = \frac{h}{V_s T_s} \tag{2}$$

and structure aspect ratio,  $h/r$ . Veletsos also found that period lengthening is a nearly unique function of  $\sqrt{\gamma\phi}$ , where  $\gamma$ =ratio of structure-to-soil mass (generally  $\approx 0.15$ ), and

$$\phi = \frac{1}{\sigma_s} \left( \frac{h}{r} \right)^{1/4} \quad (3)$$

Stewart et al. (1999) evaluated inertial interaction effects empirically using parametric system identification analyses of building response, and confirmed that period lengthening correlates well with  $l/\sigma_s$ . Inertial interaction effects were found to be nearly negligible for  $l/\sigma_s < 0.1$ , but significant for  $l/\sigma_s > 0.1$  to 0.15.

To investigate the effect of inertial interaction on foundation/free-field ground motion variations, the database with  $e/r < 0.5$  was sorted using parameters  $l/\sigma_s$ ,  $\phi$ , and number of stories. The sort using number of stories was motivated by its use as an index for inertial interaction in current strong motion selection procedures for attenuation relations.

In order to investigate the effect of number of stories on foundation/free-field ground motion variations, the database with  $e/r < 0.5$  is plotted in Figure 4a with the data sorted into bins with  $\leq 3$  stories and  $> 3$  stories. Regressions according to Equation 1 are also plotted in Figure 4a. Standard error terms for data in the two bins are compared to those for the full data set with  $e/r < 0.5$  in Table 4. Since the intent here is the evaluation of inertial interaction effects, emphasis is given to the  $S_a @ \tilde{T}$  data in interpretation of results from Figure 4a and Table 4. Two observations are made from this table and figure:

- The regression results indicate no significant differences in MHA or  $S_a @ \tilde{T}$  for buildings in the two bins.
- The standard error from the bin with  $\leq 3$  stories exceeds that for the overall data set and the bin with  $> 3$  stories. Since, the bin with  $\leq 3$  stories represents a more restricted set of conditions (buildings with only 1 to 3 stories) than the bin with  $> 3$  stories (buildings with 4 to 31 stories), the opposite would be expected if number of stories is a good index for inertial interaction.

These results suggest that number of stories may not be the optimal parameter for the evaluation of inertial interaction, although it is recognized that the scatter in the data is sufficient that trends are difficult to identify.

In Figure 4b, the database with  $e/r < 0.5$  is plotted with the data sorted into bins with  $l/\sigma_s < 0.1$  and  $l/\sigma_s > 0.1$  along with regressions according to Equation 1. The results indicate that motions from buildings with  $l/\sigma_s > 0.1$  are larger than motions from buildings with negligible inertial interaction. Although these differences are small with respect to data scatter, the trend suggests that structural vibrations may be enhancing foundation motions in buildings with significant inertial interaction, which is expected. A sort with  $\phi < 0.1$  and  $\phi > 0.1$  (results not shown except for standard error values in Table 4) yielded very similar results to those shown in Figure 4b. Since adding  $h/r$  to the inertial interaction index (i.e., using  $\phi$  vs.  $l/\sigma_s$ ) did not improve the results,  $l/\sigma_s$  is adopted as the index for inertial interaction effects on foundation translational motion.

Standard errors for  $S_a @ \tilde{T}$  data in the different  $l/\sigma_s$  bins (Table 4) indicate that the well constrained bin with small inertial interaction ( $l/\sigma_s = 0-0.1$ ) has less scatter than the complete data set, whereas the less constrained bin with large inertial interaction ( $l/\sigma_s = 0.1-0.3$ ) has more scatter. These results suggest that  $l/\sigma_s$  is a reasonable index for inertial interaction, and that  $l/\sigma_s = 0.1$  is a limiting value beyond which inertial interaction effects can be expected to add uncertainty to the data. However, since the data in Figure 4b indicates that the effect of

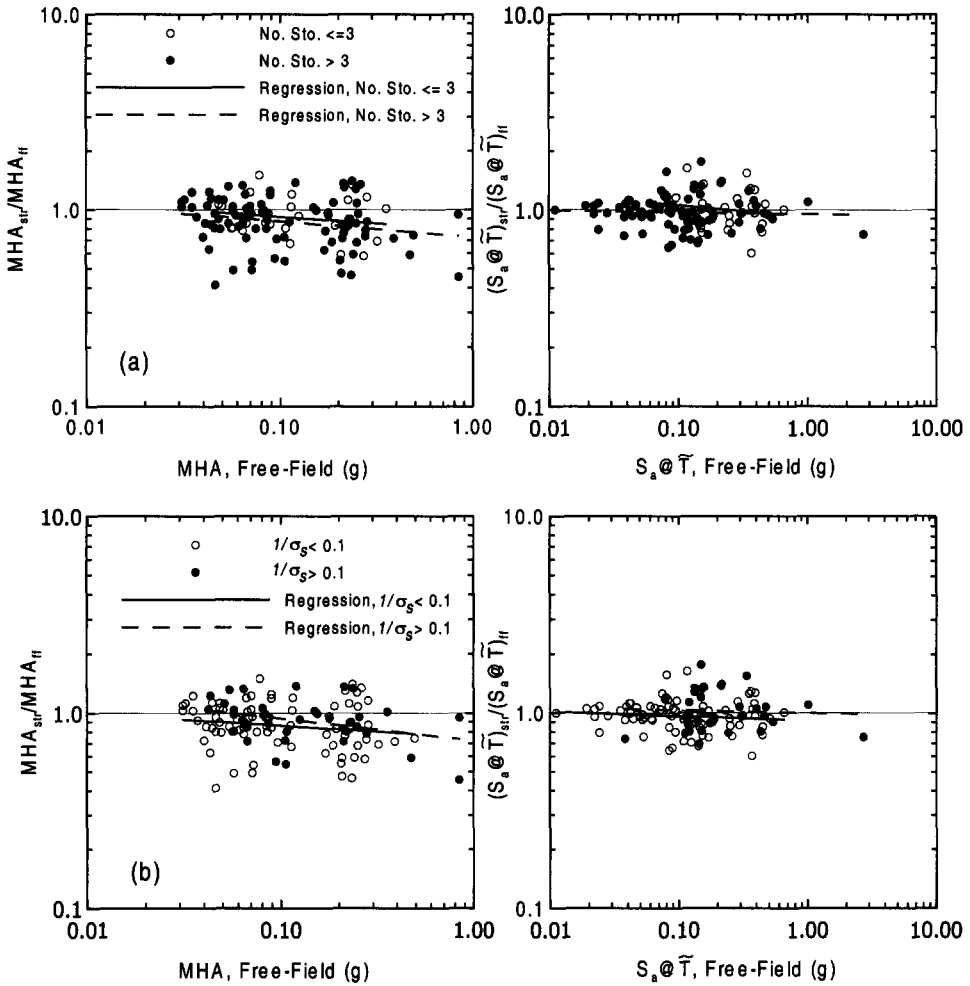


Figure 4. Ratio of foundation-level/free-field motion, data set with  $e/r < 0.5$  sorted according to (a)  $\leq 3$  stories and  $> 3$  stories and (b)  $1/\sigma_s < 0.1$  and  $1/\sigma_s > 0.1$ .

Table 4. Error terms for  $e/r < 0.5$  and different data bins for number of stories and  $1/\sigma_s$ .

Bin	# data pts.	$\sigma$ (MHA)	$\sigma$ ( $S_a @ \tilde{T}$ )
Data set with $e/r < 0.5$	117	0.267	0.200
No. Stories $\leq 3$	28	0.232	0.219
No. Stories $> 3$	89	0.277	0.192
$1/\sigma_s < 0.1$	81	0.273	0.182
$1/\sigma_s > 0.1$	36	0.247	0.231
$\phi < 0.1$	85	0.273	0.185
$\phi > 0.1$	32	0.248	0.231

inertial interaction on foundation/free-field ground motion variations is fairly small, subsequent data analysis will in general not remove results for buildings with  $l/\sigma_s > 0.1$ .

### BASE SLAB AVERAGING

Veletsos and Prasad (1989) and Veletsos et al. (1997) investigated with theoretical analyses base slab averaging effects for rigid foundations subjected to nonvertically incident and incoherent wave fields. It was found that the filtering of translational motion on base slabs increases with dimensionless frequency,  $\tilde{a}_0$ , defined for circular foundations as,

$$\tilde{a}_0 = \frac{\omega r}{V_s} \sqrt{\kappa^2 + \sin^2 \alpha_v} \quad (4)$$

where  $\omega$ =circular frequency,  $r$  = foundation radius,  $\kappa$ =an incoherence parameter for the incident waves, and  $\alpha_v$ =vertical angle of incidence of waves. For analysis of translations on non-circular foundations,  $r$  can be calculated from the area of the actual foundation ( $\sqrt{A_f/\pi}$ ) without introduction of significant error (Veletsos et al., 1997). Kim and Stewart (2000) examined complete foundation/free-field transfer functions for the sites with  $e/r < 0.5$  in Table 2 in order to calibrate the  $\kappa$  parameter assuming  $\alpha_v = 0$ . Values of  $\kappa$  obtained from these analyses are presented in Table 2. Since actual foundations are non-rigid, and the filtering of foundation motion includes contributions from inclined waves and wave scattering effects in addition to base slab averaging, these  $\kappa$  values provide only a first-order approximation of true base slab averaging effects.

Kinematic interaction effects for shallow foundations are investigated here using  $\tilde{a}_0$  as an index parameter. Using  $\kappa$  values from Table 2 and  $\alpha_v = 0$ ,  $\tilde{a}_0$  values were computed for each site at the following spectral periods: 0.18, 0.32, 0.56, 1.0, 1.8, and 3.0 s. The resulting range of  $\tilde{a}_0$  for sites in the database is ~0 to 1.7. Foundation-level and free-field 5% damped spectral accelerations computed at these same spectral periods are compiled in Figure 5a for the data set with  $e/r < 0.5$  sorted according to  $\tilde{a}_0 < 0.2$  and  $\tilde{a}_0 > 0.5$ , along with regressions from Equation 1. The results indicate a significantly greater level of de-amplification for  $\tilde{a}_0 > 0.5$  than for  $\tilde{a}_0 < 0.2$ . Standard errors for various bins of  $\tilde{a}_0$  and the full data set are presented in Table 5. Data scatter is seen to increase generally with  $\tilde{a}_0$ , and significant benefit (in the form of uncertainty reduction) is gained by maintaining  $\tilde{a}_0 < 0.2$ . The data in Figure 5a and Table 5 suggests that accepting into databases only data with  $\tilde{a}_0 < 0.2$  may be a reasonable way of controlling base slab averaging effects.

Since the results in Figure 5a are compiled over a range of spectral periods, they largely reflect the influence of frequency on foundation/free-field ground motion variations. To investigate the influence of other parameters controlling base slab averaging such as  $r$ ,  $\kappa$ , and  $V_s$ , foundation/free-field ratios for  $T=0.18$  s and 1.0 s with sorting according to  $\tilde{a}_0/\omega < 0.02$  s and  $\tilde{a}_0/\omega > 0.02$  s are presented in Figure 5b. This limiting value of  $\tilde{a}_0/\omega$  roughly corresponds to  $\tilde{a}_0 = 0.7$  for  $T=0.18$  s and  $\tilde{a}_0 = 0.12$  for  $T=1.0$  s. The strong influence of frequency on foundation motion de-amplification is clear, as foundation/free-field ratios are nearly one for  $T = 1.0$  s but significantly less than one for  $T = 0.18$  s. However, the data also indicate that foundation motion filtering increases with increasing  $\tilde{a}_0/\omega$  in both the  $T = 0.18$  s

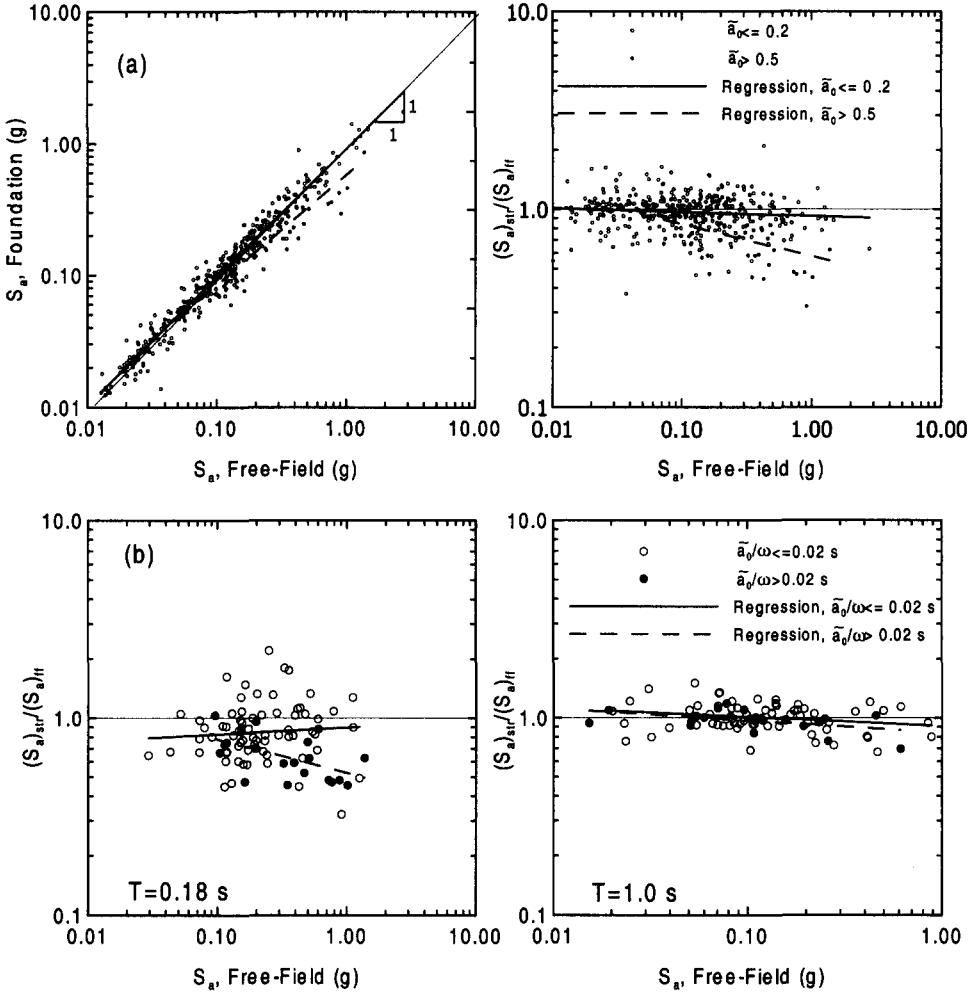


**Figure 5.** Variation between free-field and foundation-level 5% damped spectral accelerations,  $e/r < 0.5$ , (a) sorted by  $\tilde{a}_0$ ; (b) sorted by  $\tilde{a}_0/\omega$ .

**Table 5.** Error terms for  $e/r < 0.5$  and different data bins for  $\tilde{a}_0$

Bin	# data pts.	$\sigma(S_a)$
Complete data set with $e/r < 0.5$	702	0.254
$\tilde{a}_0 \leq 0.2$	395	0.202
$\tilde{a}_0 = 0.2-0.5$	99	0.315
$\tilde{a}_0 = 0.4-0.6$	46	0.273



and  $T=1.0$  s data sets. This result confirms that factors other than frequency (i.e.,  $V_s$ ,  $\kappa$ , and  $r$ ) in the expression for  $\tilde{a}_0$  contribute to foundation motion de-amplification. Therefore, there appears to be value in retaining  $\tilde{a}_0$  over frequency as an index for base slab averaging.

## SUMMARY

The previous sections have outlined the influence of several key factors on the ratio of foundation/free-field motion. In their approximate order of importance, these include embedment ratio  $e/r$ , dimensionless frequency  $\tilde{a}_0$ , and ratio of structure-to-soil stiffness  $1/\sigma_s$ . The effects of these various parameters are summarized in Figure 6 and outlined below:

Figure 6a presents on the same plot ratios of spectral acceleration computed at  $T=0.18, 0.32, 0.56, 1.0, 1.8,$  and  $3.0$  s for the complete data set, along with regression results according to Equation 1. The regression indicates de-amplification of foundation translations for free-field spectral accelerations larger than about  $0.1g$ , and the error term is fairly large ( $\sigma=0.261$ ).

The effects of removing data from deeply embedded structures ( $e/r > 0.5$ ) are shown in Figure 6b. The error term is reduced only slightly to  $\sigma=0.254$  (due to the relatively small number of deeply embedded structures in the database), but the regression indicates that the spectral acceleration ratios are somewhat closer to one.

The effects of removing data with high normalized frequencies,  $\tilde{a}_0 > 0.2$ , are shown in Figure 6c. The error term is reduced substantially to  $\sigma=0.202$ , and the regression indicates spectral acceleration ratios that are now fairly close to one.

The effects of removing data from structures subject to significant inertial interaction effects,  $1/\sigma_s > 0.1$ , are shown in Figure 6d. There is no appreciable change from the results in Figure 6c, either in standard error or spectral acceleration ratio. This does not imply, however, that inertial interaction effects cannot influence foundation-level recordings. Structures with significant inertial interaction tend to have high fundamental-mode frequencies, and the foundation-level ground motion amplification at these frequencies is largely removed with the omission of  $\tilde{a}_0 > 0.2$  data in the previous step.

## IMPLICATIONS FOR ATTENUATION RELATIONS

### SPECTRAL ACCELERATION

Based on the above findings, some modifications to procedures for screening structural recordings for use in attenuation relations may be appropriate. Current procedures use properties such as number of basement levels, number of stories, and "massive" vs. "non-massive" foundations as indices for soil-structure interaction effects. The first two of these were addressed through this study, and it was found that  $e/r$  and  $1/\sigma_s$  are improved parameters describing embedment and inertial effects, respectively. Another factor investigated here, but which is not considered in present selection procedures, is normalized frequency,  $\tilde{a}_0$ . This factor represents a useful index for base slab averaging effects, which can be significant at high frequencies ( $\tilde{a}_0 > 0.2$ ). The foundation mass of buildings in this study is typical of ordinary building construction in California, and would generally not be considered "massive." Hence, an empirical assessment of ground motion variations between "massive" and "non-massive" foundations was not possible.

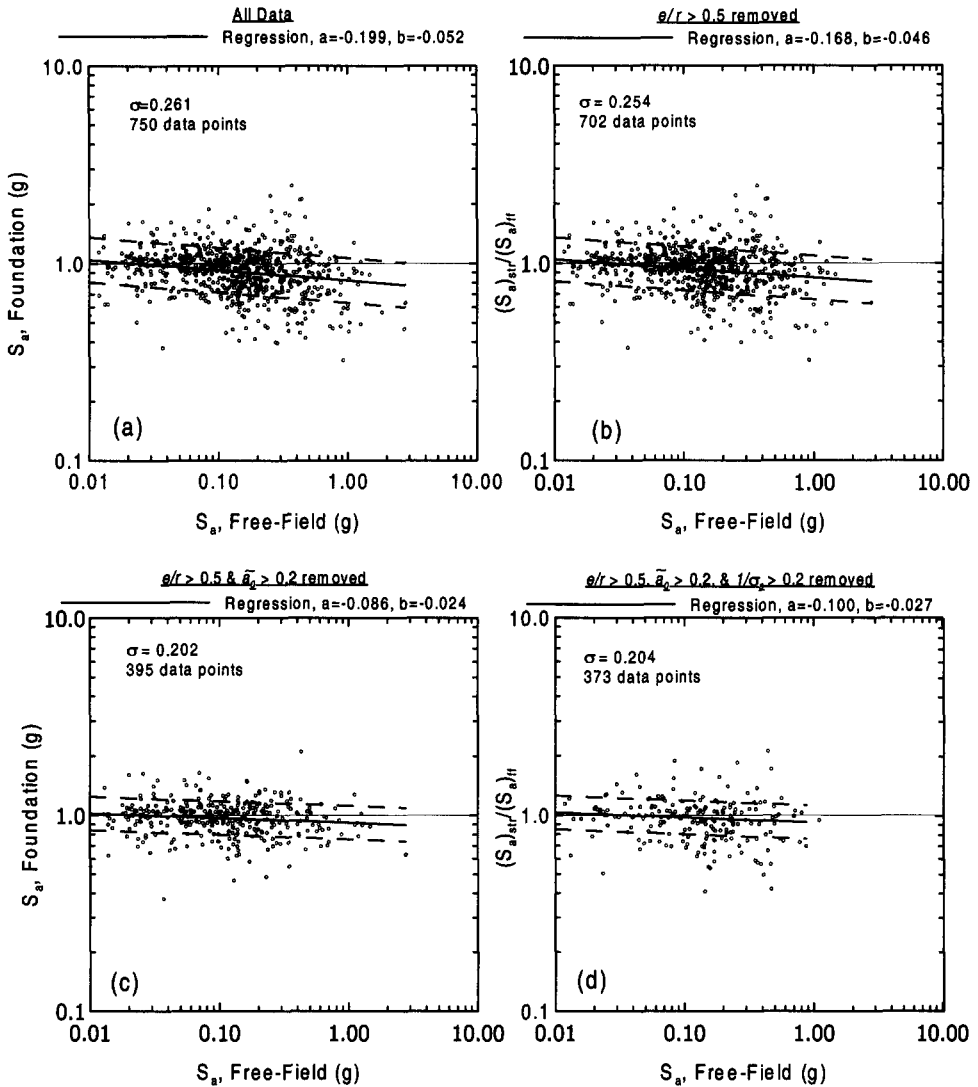


**Figure 6.** Summary of foundation/free-field ratios of 5% damped spectral accelerations, sorting by  $e/r$ ,  $\tilde{a}_0$ , and  $1/\sigma$ .

In adopting foundation-level recordings as representative of free-field conditions, the principal considerations are:

1. Do the amplitudes of foundation and free-field motions differ significantly, i.e., is the median foundation/free-field ratio of spectral accelerations nearly one?
2. Does the addition of foundation-level motions to strong motion databases significantly increase the scatter or uncertainty in regression analyses?

Typical error terms from attenuation relations are on the order of 0.4 to 0.9, which is considerably larger than error terms for foundation/free-field ratios identified here ( $\sim 0.2$ ). Hence, perhaps the most critical concern is avoiding systematic bias in foundation-level motion relative to free-field motion. To minimize this bias, it is recommended that data be

selected only from shallowly embedded structures with  $e/r < 0.5$ , and that only spectral ordinates with low normalized frequencies ( $\tilde{a}_0 < 0.2$ ) be used. Available data suggests that further screening for inertial interaction effects may not be necessary. Nonetheless, for buildings with  $l/\sigma_s > 0.1$ , a wise practice would be to avoid the use of components of foundation-level recordings near the fundamental-mode building frequency, as they are likely to be amplified (fortunately, such components are often removed by the  $\tilde{a}_0$  criteria).

Some investigators may find the  $\tilde{a}_0$  and  $l/\sigma_s$  selection criteria outlined above overly cumbersome for practical application. As the effect of  $l/\sigma_s$  on spectral acceleration ratios is modest, and the effect of  $\tilde{a}_0$  is largely related to spectral period, useful insights might be anticipated from simple statistical analyses on spectral acceleration ratios at various spectral periods. Accordingly, single median values of spectral acceleration ratio and standard error terms were evaluated at spectral periods  $T=0.18, 0.32, 0.56, 1.0, 1.8,$  and  $3.0$  s using data sorted only according to  $e/r < 0.5$ . The results are compiled in Figure 7, and show decreasing bias and standard error with increasing spectral period up to  $T = 1.0$  s. These results suggest that for  $T \geq \sim 1.0$  s, median foundation-level spectral accelerations are within about 1 to 3 percent of free-field spectral accelerations, and that the standard error of the ratio is small ( $\sigma \approx 0.18$  to  $0.22$ ). This finding is consistent with Campbell (1984a), who also found negligible de-amplification for spectral periods larger than 1 s.

#### OTHER GROUND MOTION PARAMETERS

Examined here are variations between foundation and free-field Maximum Horizontal Velocity (MHV) and Maximum Vertical Acceleration (MVA). Ground motion attenuation relations for MHV and MVA have been developed by Campbell (1997).

Plotted in Figure 8a are foundation/free-field ratios of MHV. Trends in the data are similar to those noted previously for MHA (Figure 3d), namely, a significantly higher level of de-amplification of foundation-level motion is observed for  $e/r > 0.5$  than for  $e/r < 0.5$ . However, the scatter in the MHV data for  $e/r < 0.5$  ( $\sigma=0.180$ ) is much smaller than in the MHA data ( $\sigma=0.267$ ) due to the more pronounced influence of low frequency components of motion on MHV. Overall, for sites with  $e/r < 0.5$ , MHV recordings from foundations appear to provide nearly unbiased estimates of free-field MHV.

Plotted in Figure 8b are foundation/free-field ratios of MVA using the data set with  $e/r < 0.5$ . The regression shows significant de-amplification of foundation-level MVA, and larger scatter ( $\sigma=0.333$ ) than the MHA data ( $\sigma=0.267$ ). Results similar to those in Figure 8d were obtained from separate regressions utilizing only data with  $e/r=0$  (not shown), hence, like MHA, these results are only moderately sensitive to  $e/r$  for  $e/r < 0.5$ . The relatively high level of scatter likely results from the following sources: (1) Vertical accelerations often have a higher frequency content than horizontal motions, and hence will be more influenced by noise effects such as spatial incoherence and will be subject to base slab averaging effects which can vary from site-to-site, and (2) Vertical motions near shear walls can be significantly influenced by rocking, and hence the results are likely sensitive to the locations of vertical instruments on foundations, which are not consistent from site-to-site. Based on the large scatter and significant de-amplification evident in Figure 8b, foundation-level MVA does not appear to provide an accurate estimate of free-field MVA.

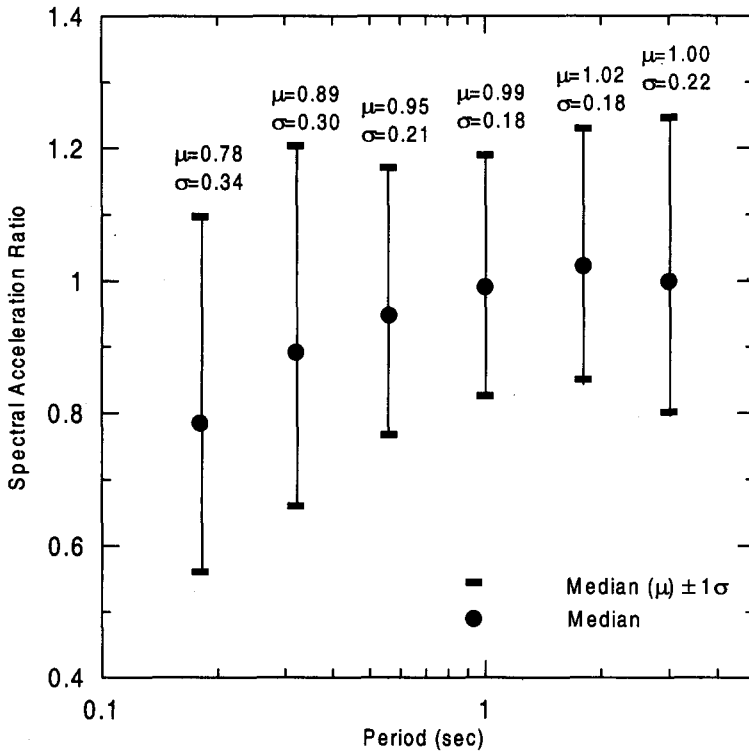


Figure 7. Statistical values of 5% damped spectral acceleration ratio for various spectral periods, data set with  $e/r < 0.5$ .

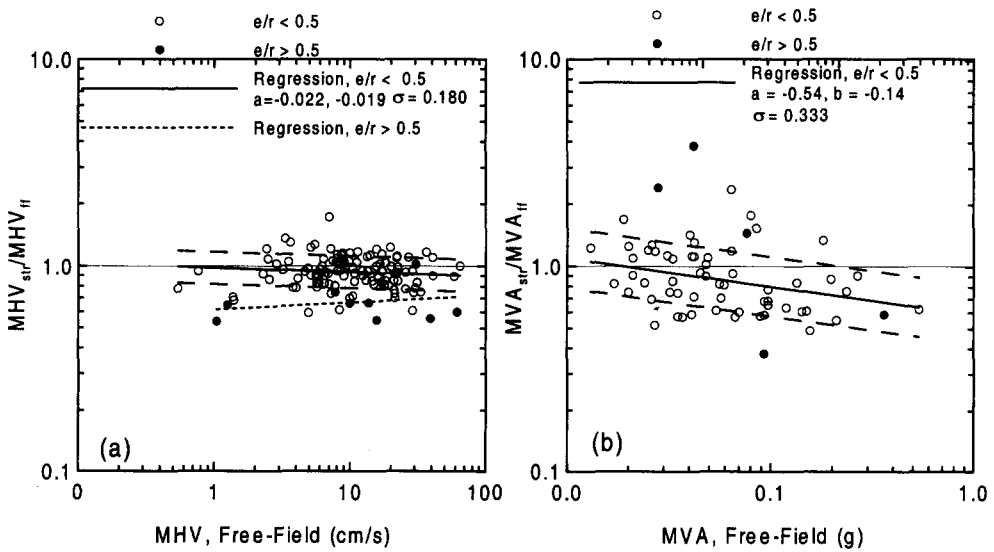


Figure 8. Foundation/free-field ratios of MHV and MVA.

## CONCLUSIONS

Variations between foundation and free-field motions can result from kinematic and inertial soil-structure interaction effects, as well as localized soil nonlinearities beneath the foundation. While inertial interaction can lead to minor amplification of foundation motion relative to the free-field, kinematic and nonlinear effects, which tend to de-amplify high frequency motions, are generally more significant. Site categorizations based on parameters that strongly influence inertial and kinematic processes were found to be capable of delineating conditions where foundation motions are representative of free-field shaking from those where biases or excessive uncertainty are present.

Based on the observations from the field performance data, it is clear that conditions exist for which horizontal foundation motion (expressed in terms of spectral accelerations) can provide a nearly unbiased estimate of horizontal free-field motion with little uncertainty. For this to be the case, the foundation should be shallowly embedded ( $e/r < 0.5$ ), and the frequency range of interest should be low ( $\tilde{\alpha}_0 < 0.2$  or, more approximately,  $T > 1$  s) and distinct from the fundamental-mode frequency of the structure. Incorporation of data meeting these criteria into regressions for attenuation relations could significantly increase the sizes of databases, especially for long-period components of motion.

## ACKNOWLEDGMENTS

The author would like to thank Drs. Kenneth Campbell, William Joyner, and Walter Silva for taking the time to discuss this topic and review this manuscript. The three anonymous reviewers of the manuscript are also thanked for their helpful comments and suggestions. Support for this project was provided by a CAREER grant from the National Science Foundation through the Earthquake Hazards Reduction Program (NSF Award No. CMS-9733113). This support is gratefully acknowledged. The views and conclusions contained in this document are those of the author and should not be interpreted as necessarily representing the official policies, either expressed or implied, of the U.S. government.

## REFERENCES CITED

- Abrahamson, N. A., 1988, Empirical models of spatial coherency of strong ground motion, *Proceedings 2nd Workshop on Strong Motion Arrays*, Institute of Earth Sciences, Taipei, Taiwan, 65-92.
- Abrahamson, N. A., Schneider, J. F., and Stepp, J. C., 1991, Empirical spatial coherency functions for application to soil-structure interaction analyses, *Earthquake Spectra*, **7** (1), 1-27.
- Abrahamson, N. A. and Silva, W. J., 1997, Empirical response spectral attenuation relations for shallow crustal earthquakes, *Seism. Res. Letters*, **68** (1), 94-127.
- Boore, D. M., Joyner, W. B., Oliver, A. A., and Page, R. A., 1980, Peak acceleration, velocity, and displacement from strong-motion records, *Bull. Seism. Soc. Am.*, **70** (1), 305-321.
- Boore, D. M., Joyner, W. B., and Fumal, T. E., 1997, Equations for estimating horizontal response spectra and peak acceleration from Western North American Earthquakes: A summary of recent work, *Seism. Res. Letters*, **68** (1), 128-153.
- Campbell, K. W., 1984a, Near-source attenuation of strong ground motion for moderate to large earthquakes—An update and suggested application for the Wasatch Fault Zone of Northcentral Utah, in *Evaluation of Regional and Urban Earthquake Hazards and Risk in Utah*, W. W. Hays and P. L. Gori (eds.), *Proceedings 26<sup>th</sup> NEHRP Workshop*, Salt Lake City, Utah, Report No. USGS OFR 84-763.

- Campbell, K. W., 1984b, Observed structural modification of recorded strong ground motion, in *Critical Aspects of Earthquake Ground Motion and Building Damage Potential*, Applied Technology Council, Report No. ATC-10-1, Palo Alto, CA, 43-52.
- Campbell, K. W., 1986, Empirical prediction of free-field ground motion using statistical regression models, in *Proceedings Soil-Structure Interaction Workshop*, Bethesda, Maryland, U.S. Nuclear Regulatory Commission, Washington, DC, 12-24.
- Campbell, K. W., 1997, Empirical near-source attenuation relations for horizontal and vertical components of peak ground acceleration, peak ground velocity, and pseudo-absolute acceleration response spectra, *Seism. Res. Letters*, **68** (1), 154-179.
- Chang, C.-Y., Power, M. S., Idriss, I. M., Somerville, P. G., Silva, W. J., and Chen, P. C., 1985, Engineering characterization of ground motion. Task 2: Observational data on spatial variations of earthquake ground motion, Report No. NUREG/CR-3805, U.S. Nuclear Regulatory Commission, Washington DC, February.
- Chopra, A. K., 1995, *Dynamics of Structures*, Prentice Hall, Upper Saddle River, NJ, p. 192.
- Day, S. M., 1978, Seismic response of embedded foundations, *Proceedings ASCE Convention*, Chicago, IL, October, Preprint 3450.
- Duke, C. M., Luco, J. E., Carriveau, A. R., Hradilek, P. J., Lastico, R., and Ostrom, D., 1970, Strong earthquake motion and site conditions: Hollywood, *Bull. Seism. Soc. Am.*, **60** (4), 1274-1289.
- Elsabee, F. and Morray, J. P., 1977, Dynamic behavior of embedded foundations, Report No. R77-33, Dept. of Civil Engrg., Massachusetts Inst. Technology.
- Housner, G. W., 1959, Interaction of building and ground during an earthquake, *Bull. Seism. Soc. Am.*, **47** (3), 179-186.
- Idriss, I. M., 1991, Procedures for selecting earthquake ground motions at rock sites, *A Report to the National Institute of Standards and Technology*, Univ. of California, Davis. (rev. Sept. 1993)
- Kim, S. and Stewart, J. P., 2000, Kinematic soil-structure interaction from strong motion recordings, *J. Geotech. & Geoenv. Engrg.*, ASCE (in review).
- Kramer, S. L., 1996, *Geotechnical Earthquake Engineering*. Prentice Hall, Upper Saddle River, NJ, 294-303.
- Kurimoto, O., and Iguchi, I., 1996, Evaluation of foundation input motions based on observed seismic motions, *Proceedings 11<sup>th</sup> World Conference on Earthquake Engrg.*, Paper 317.
- Lee, V. W., Trifunac, M. D., and Feng, C. C., 1982, Effects of foundation size on Fourier spectrum amplitudes of earthquake accelerations recorded in building, *Soil Dyn. Eq. Engrg.*, **1** (2), 52-58.
- Lee, V. W. and Trifunac, M. D., 1996, Characteristics of earthquake response spectra in southern California, Report to California Dept. of Transportation, and City and County of Los Angeles, Southern California Earthquake Center, Los Angeles, CA.
- McCann, M. W. and Boore, D. M., 1983, Variability in ground motions: Root mean square acceleration and peak acceleration for the 1971 San Fernando, California, earthquake, *Bull. Seism. Soc. Am.*, **73** (2), 615-632.
- Moslem, K. and Trifunac, M. D., 1987, Spectral amplitudes of strong earthquake accelerations recorded in buildings, *Soil Dyn. Eq. Engrg.*, **6** (2), 100-107.
- Newmark, N. M., Hall, W. J., and Morgan, J. R., 1977, Comparison of building response and free field motion in earthquakes, *Proceedings 6th World Conference on Earthquake Engrg.*, Sarita Prakashan, Meerut, India, Vol. II, 972-978.
- Sadigh, K., Chang, C.-Y., Egan, J. A., Makdisi, F., and Youngs, R. R., 1997, Attenuation relationships for shallow crustal earthquakes based on California strong motion data, *Seism. Res. Letters*, **68** (1), 180-189.
- Scanlan, R. H., 1976, Seismic wave effects on soil-structure interaction, *Earthquake Engrg. and Struct. Dynamics*, **4**, 379-388.

- Seed, H. B. and Lysmer, J., 1980, The seismic soil-structure interaction problem for nuclear facilities, in *Soil-structure interaction: The status of current analysis methods and research*, J.J. Johnson, ed., *Report No. NUREG/CR-1780 and UCRL-53011*, U.S. Nuclear Regulatory Com., Washington DC and Lawrence Livermore Lab., Livermore, CA.
- Seismological Research Letters*, 1997, Special issue on ground motion attenuation relations. **68** (1). January/February.
- Stewart, J. P., 1996, An empirical assessment of soil-structure interaction effects on the seismic response of structures, *Ph.D. Dissertation*, U.C. Berkeley.
- Stewart, J. P. and Kim, S., 1998, Empirical verification of soil-structure interaction provisions in building codes, in *Geotechnical Earthquake Engineering and Soil Dynamics-III*, ASCE Geotechnical Special Publication No. 75, P. Dakoulas, M. Yegian, and R. D. Holtz (editors), 1259-1270.
- Stewart, J. P., Seed, R. B., and Fenves, G. L., 1999, Seismic soil-structure interaction in buildings. II: Empirical results, *J. Geotech. & Geoenv. Engrg.*, ASCE, **125** (1), 39-48.
- Stewart, J. P. and Stewart, A. F., 1997, Analysis of soil-structure interaction effects on building response from earthquake strong motion recordings at 58 sites, *Report No. UCB/ERC-97/01*, Earthquake Engrg. Research Ctr., Univ. of California, Berkeley, 742 pp.
- Trifunac, M. D., 1972, Interaction of a shear wall with the soil for incident plane SH waves, *Bull. Seism. Soc. Am.*, **62** (1), 63-83.
- Trifunac, M. D., 1976a, Preliminary analysis of the peaks of strong earthquake ground motion-Dependence of peaks on earthquake magnitude, epicentral distance, and recording site conditions, *Bull. Seism. Soc. Am.*, **66** (1), 189-219.
- Trifunac, M. D., 1976b, Preliminary empirical model for scaling Fourier amplitude spectra of strong ground acceleration in terms of earthquake magnitude, source-to-station distance, and recording site condition, *Bull. Seism. Soc. Am.*, **66** (4), 1343-1373.
- Trifunac, M. D. and Todorovska, M. I., 1996, Nonlinear soil response – 1994 Northridge, California, earthquake, *J. Geotech. & Geoenv. Engrg.*, ASCE, **122** (9), 725-735.
- Veletsos, A. S., 1977, Dynamics of structure-foundation systems, *Structural and Geotechnical Mechanics*, Prentice-Hall, Inc., Englewood Cliffs, NJ, 333-361.
- Veletsos, A. S. and Prasad, A. M., 1989, Seismic interaction of structures and soils: stochastic approach, *J. Struct. Engrg.*, ASCE, **115** (4), 935-956.
- Veletsos, A. S., Prasad, A. M., and Wu, W. H., 1997, Transfer functions for rigid rectangular foundations, *J. Earthquake Engrg. Struct. Dynamics*, **26** (1), 5-17.
- Yamahara, H., 1970, Ground motions during earthquakes and the input loss of earthquake power to an excitation of buildings, *Soils and Foundations*, **10** (2), 145-161.